Fusion Engineering Hydra Hexacopter Test

T. Koning, N. Perugu

October, 2022

Abstract

This report describes the testing process of the Hydra: a hexacopter drone platform. It is to be used for the collection of official flight test results. The tests are designed to analyse the functional aspects of the Fusion Reflex flight controller. All tests are completed succesfully.

---

1. Introduction

1.1. Fusion Engineering's Reflex

Fusion Engineering's goal is to create the most reliable, flexible and easy-to-use flight controller that can be used on any type of multirotor drone: the Fusion Reflex. Whereas conventional flight controllers use Proportional-Integral-Derivative (PID) control, the Reflex uses a technique based on Incremental Non-linear Dynamic Inversion (INDI). This is a novel method designed at Delft University of Technology (TU Delft). While control algorithms such as Non-linear Dynamic Inversion (NDI) are extremely sensitive to inaccuracies in system models, INDI overcomes this shortcoming by using sensors to reduce its dependency on accurate system models. It is a more robust algorithm which also allows for precise and fast responses.

1.2. Experiment goal

The goal of this experiment is to analyse the behaviour of the Reflex in flight while mounted on the Hydra, a large hexacopter. We want to verify essential safety modes and test flight stability, as well as position accuracy while hovering and while following trajectories.

2. Equipment

2.1. Drone overview

The focus of this experiment is on the Fusion Hydra drone. The Fusion Hydra is a copy of the NLR Hydra drone. It will function as a testing platform for the Fusion Reflex flight controller.

The maximum take off weight is 5 kg. The drone frame is a carbon fiber frame using a split deck configuration. The bottom deck houses the Power Distribution Board (PDB), 5V regulator, volt/current sensor and Lidar sensor. The top deck is a mount for the Global Navigation Satellite System (GNSS) sensor module, with a L1-band patch antenna (with its base plate) and a magnetometer mounted 10 cm above the top deck on custom 3D-printed mounts. The Reflex flight controller is also mounted on the top deck using a custom 3D-printed vibration damping mount. The drone is powered by a 6S 10000 mAh battery strapped to a platform below the bottom deck with a Velcro strap.

2.2. Components

The Reflex has an IMU and a barometer for internal sensors. The PDB is a custom-made printed circuit board (PCB) that accepts battery voltage. The PDB splits the incoming power from the battery to all the motors and steps down the voltage to provide a clean 5 V supply for the Reflex and all the sensors. The external components used on this drone are:

1. HolyBro v3 telemetry radio
2. Garmin LIDAR-Lite V3
3. A voltage/current sensor
4. Ublox C94-M8P-2 developer board GNSS module
5. T-Motor MN501-S KV300 motors
6. Drotek RM3100 magnetometer
7. T-Motor F35A 3-6S BLHeli_32 ESCs

These components and their placements are demonstrated in figures 1 and 2. As the ESCs are encased in a cover underneath the motors, they are not seen in these images. Additionally, the voltage/current sensor is present but not fully visible on the bottom deck.
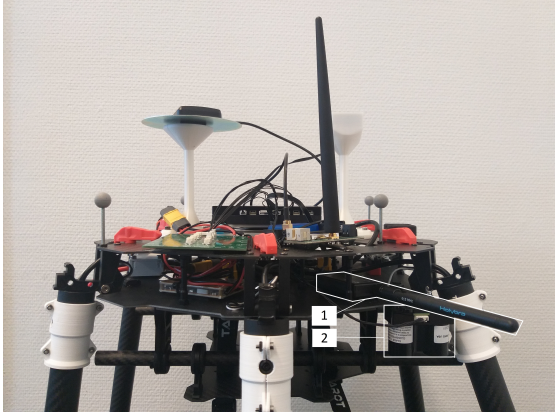
Figure 1: Hydra: side view
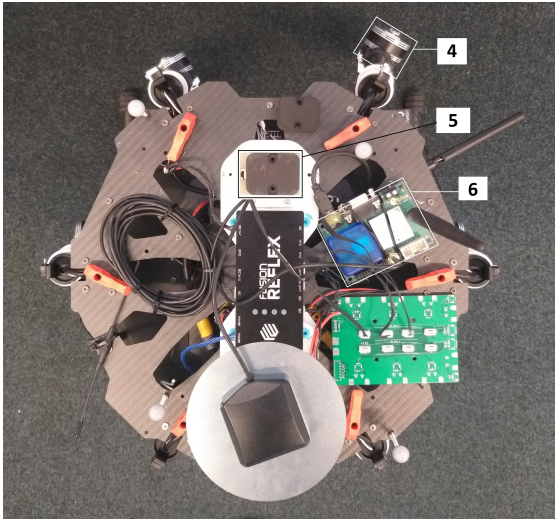
Figure 2: Hydra: top view

3. Experiments and metrics

To analyse the performance of the flight controller and determine if the tests have been completed successfully, each experiment was assigned a metric with corresponding outer bounds that the drone has to stay within.

3.1. Attitude Response

In order to test multiple aspects of the flight controller, it is necessary to ensure that the innermost control loop that stabilises the attitude of the drone is stable. This should have a maximum overshoot of 5° when a step input of 20° is applied in both roll and pitch directions. This condition is stated in equation 1.

$$O_{max} < 5[°] \mid step = 20[°] \qquad (1)$$

The step inputs must be applied 10 times in roll, and 10 times in pitch direction while alternating between back and forth motions in both cases.

They will be performed in INDI for one set and PID for another.

3.2. Position Hold

To analyse the position hold behaviour, the drone is made to hover in place. According to the Air-Tub specifications, the drone can have a maximum deviation of 20 cm from its trajectory.

$$\Delta_{pos} < 0.20[m] \qquad (2)$$

Position hold is to be tested by taking off and then centering both the remote control sticks when the drone is in the air. Position hold mode creates a position setpoint at the location where the sticks are centered. The position is held for a duration of five minutes. Position hold is tested in both INDI and PID.

3.3. GNSS Loss

If the drone loses position information from the GNSS, the uncertainty of its position will increase, resulting in inaccurate position information. Therefore, as soon as position information is lost, the drone should not try to track position anymore. The Reflex carries out this function by setting the flight mode one level lower from position mode to altitude mode.

To verify the functionality of mode switching, the drone must be flown in position mode while it holds its position. While holding position, the GNSS service will be stopped mid-flight. After shutting down the service, the position estimation expected to start fluctuating, and the flight mode should jump from position mode (2.0) to altitude mode (1.0).

3.4. Lidar Loss

The drone can get vertical position information from the internal barometer, external lidar and/or external GNSS. Whenever external sensors fail, the drone should still be able to land autonomously. For that autonomous landing, the barometer should be enough to have stable altitude information, and the controls should not automatically get pushed back to attitude flight mode because of the unreliable data.

To test this, the drone is flown in altitude mode while holding altitude, after which we shut down the sensor service that the lidar is connected to mid-flight. The drone is expected to still hold altitude, however with an increasing deviation due to the lack of the precision provided by the lidar.

2

3.5. Remote Control Loss

Whenever remote control (RC) loss occurs, the drone goes into 'RC failsafe mode'. The drone has two autonomous failsafes to choose from: 'Land' and 'Return to home and land'. In this experiment we choose the latter.

To test RC loss, the drone shall be placed in position hold, after which the RC is shut down. The commander is expected to initiate the return to home procedure: the drone must climb to a pre-defined altitude (3 m, in this case) after which the home position in x- and y-coordinates will be set as the target. Once above the home position, the drone will start to descend. The experiment is repeated twice within the same flight.

3.6. Geofence Breach

The geofence is specified as a cylinder with radius r and height h around the takeoff location. Whenever the drone breaches these boundaries of the cylinder, the drone will start its autonomous return to home procedure. The condition for this is given in equation 3.

$$if(\sqrt{x^2 + y^2} > r) \vee (z > h) : RTH \qquad (3)$$

3.7. Automated Trajectories

The AirTub project has an experiment where the drone flies over the surface of a wind turbine blade. The safe flight envelope for this manoeuvre has room for a vertical position error of $\Delta_{z,max} = 0.20[m]$. This is taken as the required boundary metric for this test.

The trajectory inputted in order to test the trajectory mode in PID and INDI is a triangle mapped out at a given altitude wherein the drone first goes west, south and then back to the origin, following which it lands.

The PID trajectory has an additional waypoint in vertical direction at 2 m. This waypoint is added to the trajectory to ensure the integrator of the vertical position PID loop has converged. Since INDI does not use an integrator, this setpoint is left out during its testing.

4. Results

The experiments for the purpose of this report were conducted in conditions with windspeeds up to 10 km/h and ambient temperatures ranging between 14° C and 19° C.

4.1. Attitude Response

The tests demonstrating the stability behaviour of the attitude responses to pitch and roll inputs were conducted in altitude mode. While using PID, the maximum overshoot observed in roll was 2.69° while the maximum overshoot in pitch was 2.10°. These occurred at timestamps of 40.66 s and 14.22 s respectively.

While piloting the drone in INDI, the the maximum overshoot observed in roll was 2.91° while the maximum overshoot in pitch was 2.73°. These occurred at timestamps of 65.24 s and 45.07 s respectively. These are all within the limit of a 5° overshoot.

4.2. Position Hold

During these experiments, the drone was made to take off and then hold its position with no stick input in position mode. The results of the experiment are visible in figures A.6 and A.7.
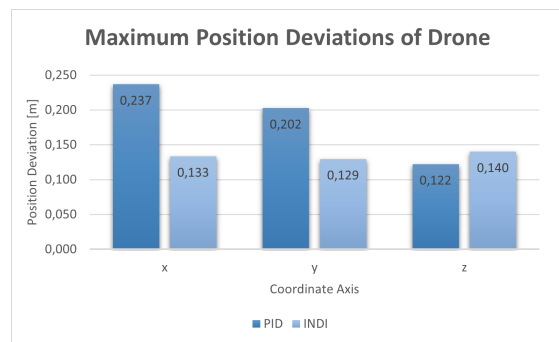
Figure 3: Linear position deviations seen in drone while flying in position hold mode.

The maximum deviations in x, y and z directions are given in figure 3. Here, it can be observed that the INDI algorithm maintains deviation lower than 20 cm in all directions whereas PID, potentially due to wind gusts, has deviations that go beyond the 20 cm limit.

4.3. GNSS Loss

The results of the GNSS loss experiment are visible in figure A.8. In the first flight, the GNSS service was stopped at the timestamp of 22.29 s while in the second flight it was stopped at 32.28 s. The standard deviation of the drone's position estimate increased rapidly following the GNSS loss due to the lack of precise position information.

The failsafe was successfully triggered in both cases wherein the flight mode switched from position (2.0) to altitude (1.0). As a result, the horizontal position was not maintained and a drifting motion was seen in the drone while it maintained its altitude.

4.4. Lidar Loss

As seen in figure A.9, the drone holds altitude quite accurately relative to the mapped setpoints with the help of the lidar. However, when the sensor service of the lidar is deactivated at 12.11 s and 14.92 s (indicated by the dotted lines), the altitude of the drone slowly begins to show larger deviation from the setpoints in the z direction.

This experiment was repeated twice. In both cases, similar behaviours were observed which, indicating that when the lidar is disabled, the barometer alone is still sufficient to maintain the altitude.

4.5. Remote Control Loss

The drone was made to take off and then hold position in position mode. The RC was then killed at time 16.83 s as seen in A.10, the failsafe was triggered and the drone entered into RTL mode. It first rose in altitude to a pre-specified height of 3 m, after which it moved towards the origin of the home position in order to descend. Partway through, the pilot took back manual control by switching to position mode at 28.08 s as seen by the purple dotted line in figure A.10.

The drone was then moved to a different xy location and once it was holding its position again, the RC was killed for the second time at time 49.24 s. The same RTL manoeuvre was executed and the drone successfully landed.

4.6. Geofence Breach

Prior to the test, the radius of the geofence was set to 10 m whereas the height was set to 5 m.

Firstly, after taking off in position mode, the geofence was breached in the radial direction at a time of 24.93 s as seen in figure A.11. The drone successfully entered into the RTL mode and began to move back toward the origin where it took off. However, at approximately the time of 35 s, the pilot took back manual control by going into position mode.

Secondly, the drone's altitude was increased until the geofence was breached in height at the time 57.12 s as seen in figure A.11. The RTL manoeuvre was fully and successfully executed and the drone landed in the position where it took off.

4.7. Automated Trajectories

The trajectory mapped out and executed in PID is demonstrated by figure A.12, whereas the results of the same manoeuvre executed in INDI are shown in figure A.13.

The maximum position deviations in PID are 15.41 cm while moving along east, 12.26 cm along north and 11.47 cm in up. In INDI, they are 9.35 cm along east, 11.11 cm along north and 10.66 cm

in up. Due to the high inertia of this large drone, such large deviations are within expectations when taking into consideration that the drone is harder to manoeuvre than a smaller one.

5. Conclusion

The purpose of the experiments conducted in this report was to analyse the behaviour of the Fusion Reflex flight controller when mounted on a large drone: the Hydra. A series of experiments were conducted in order to validate the flight controller's properties and functions.

The Reflex's failsafe protocols were first tested. A simulated GNSS loss successfully lead the flight mode to switch from position to altitude mode. Upon lidar loss, the flight controller maintained altitude using its internal barometer but larger deviations were observed than when lidar is available. RC loss and geofence breaches both successfully triggered the RTL failsafe and the manoeuvre was carried out to completion.

The stability of the attitude responses of the drone were tested for PID and INDI control algorithms. In both cases, the maximum overshoot observed in pitching and rolling motions remained below $5°$, with the maximum overshoots were both observed in roll with $2.69°$ in PID and $2.91°$ INDI.

The deviations observed in the drone while it held position were all less than 20 cm for INDI. However, for PID, the position deviations from their set points in the x and y directions were slightly larger than 20 cm at values of 23.7 cm and 20.2 cm respectively. Automated trajectories were carried out with the maximum deviation in PID being 15.41 cm along east and in INDI, the maximum being 11.11 cm along north.

For further testing and validation of the Fusion Reflex flight controller's functions, larger drones will be used as testing platforms.

4

Appendix A. Appendix A

Appendix A.1. Roll Pitch
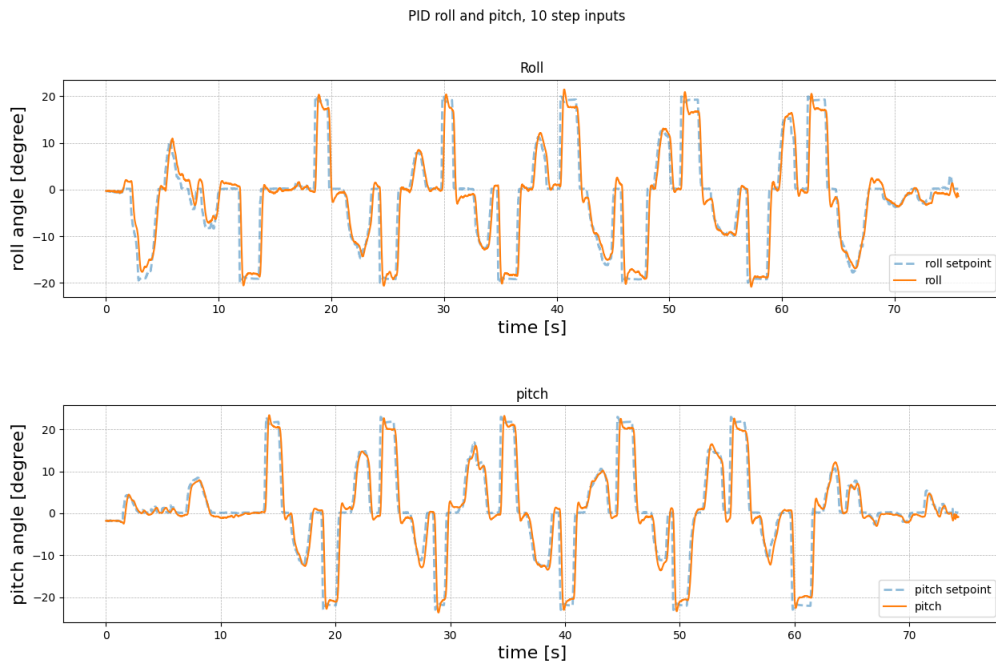
Figure A.4: PID roll pitch
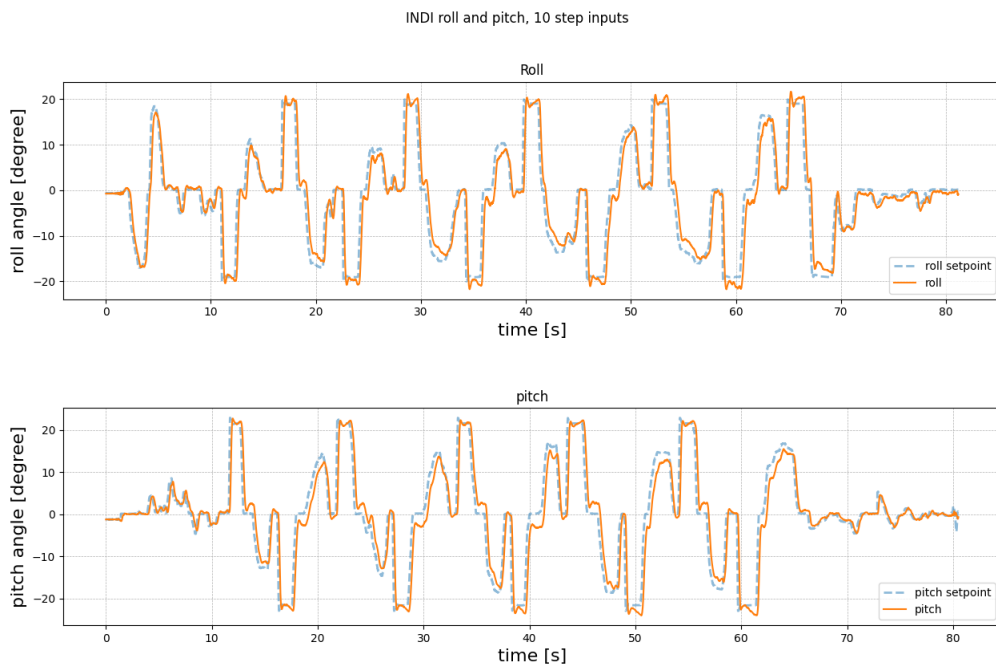
Figure A.5: INDI roll pitch

Appendix A.2. Position hold
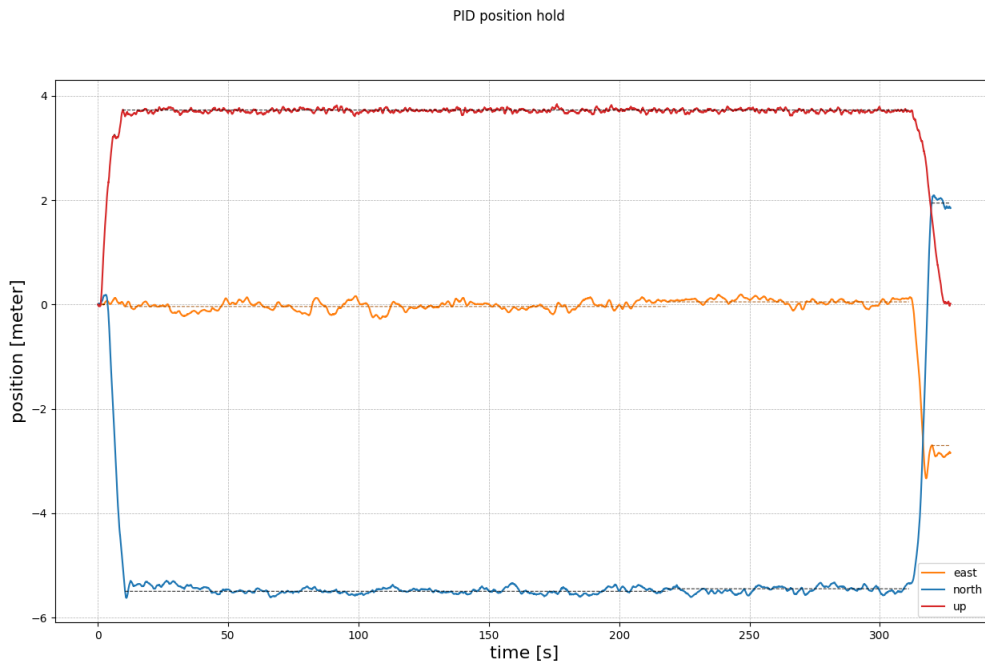
PID position hold

Figure A.6: PID position hold
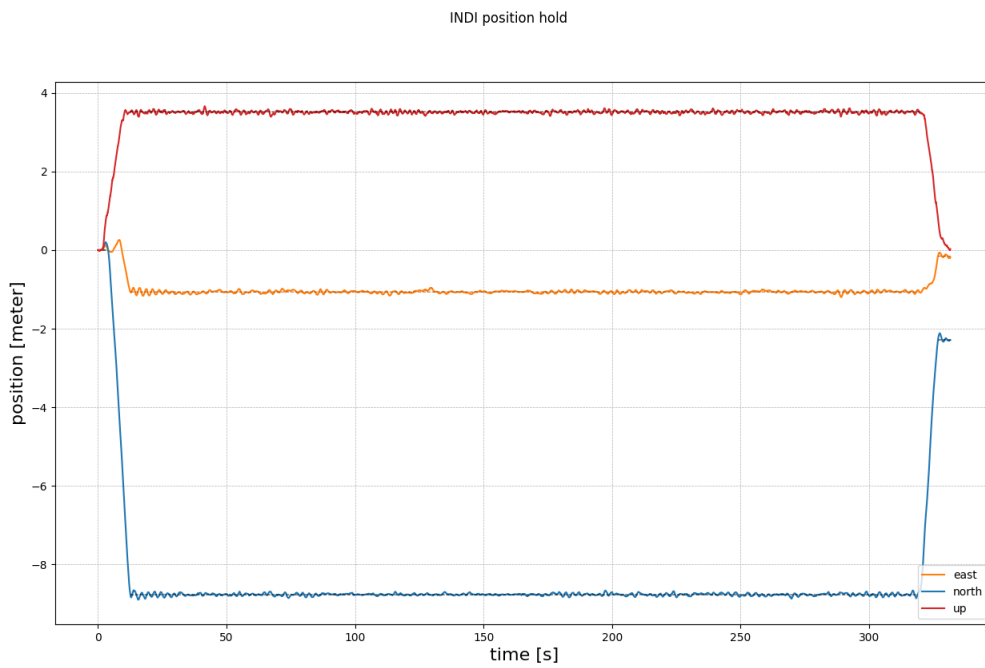
INDI position hold

Figure A.7: INDI position hold

Appendix A.3. Sensor loss

GNSS loss
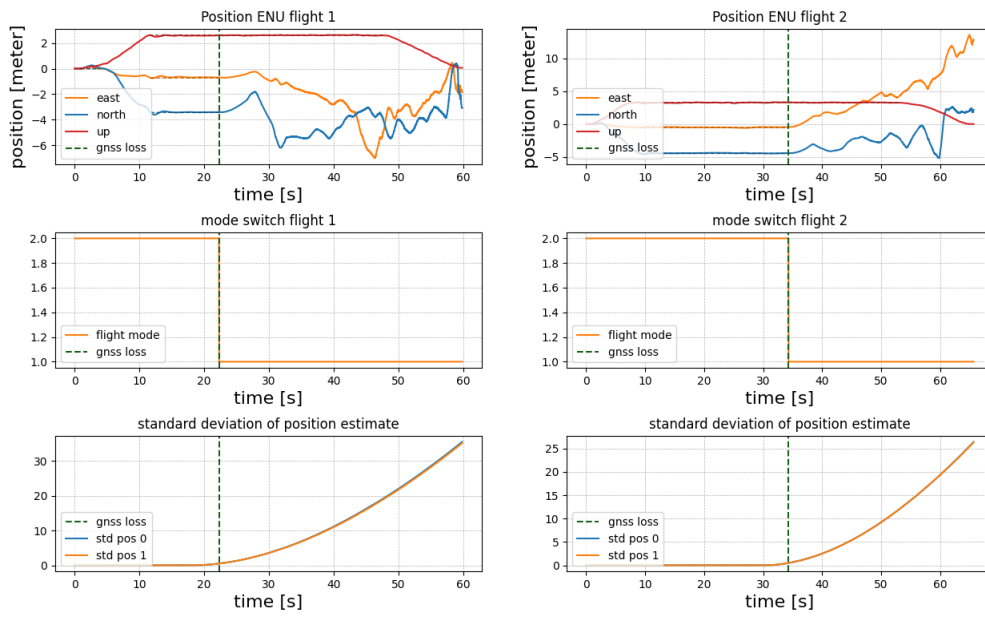
Figure A.8: GNSS loss

Lidar loss
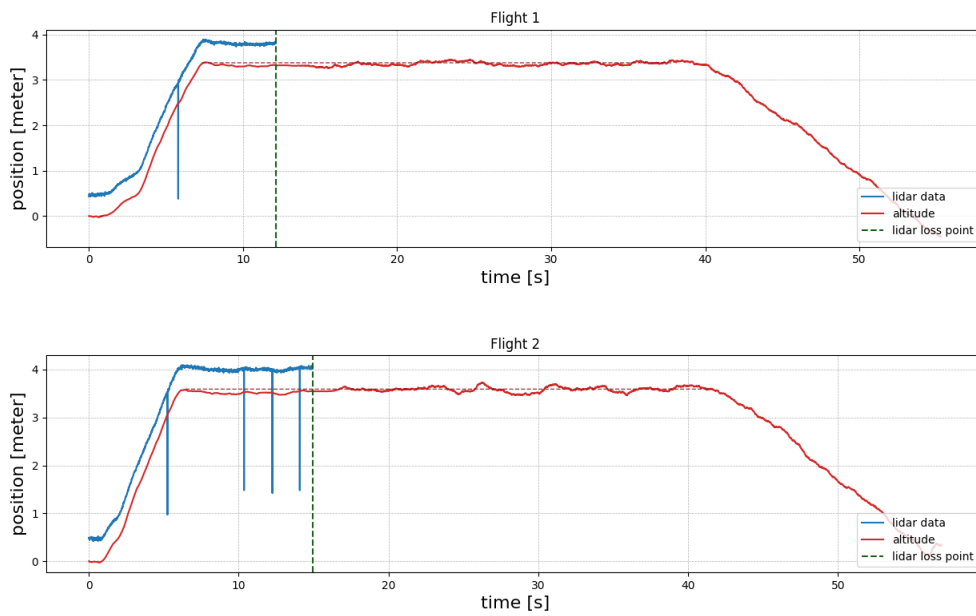
Figure A.9: Lidar loss

RC loss failsafe
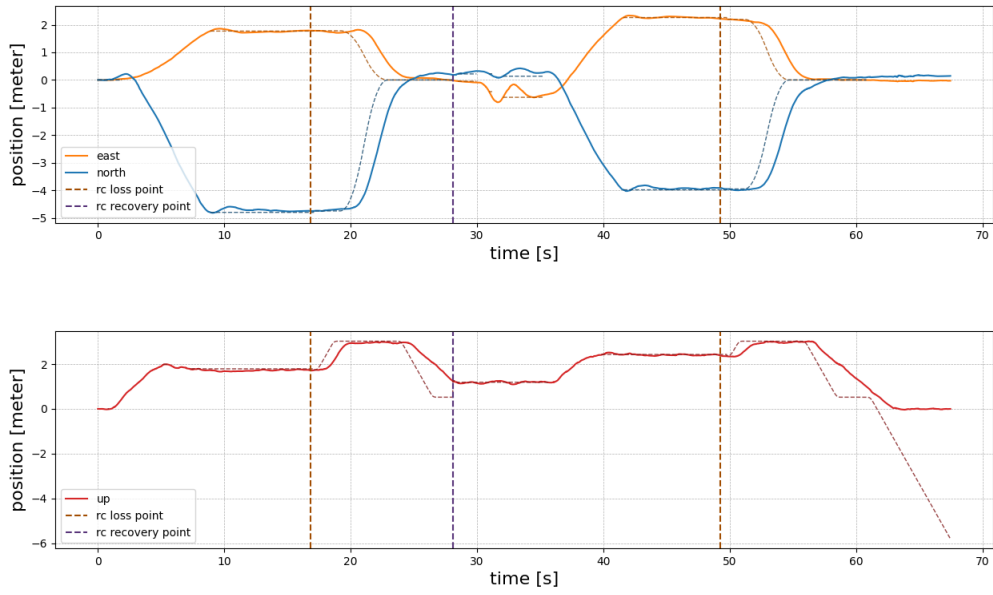
Figure A.10: RC loss

Appendix A.4. Geofence breach

Geofence breach radius of 10 meters
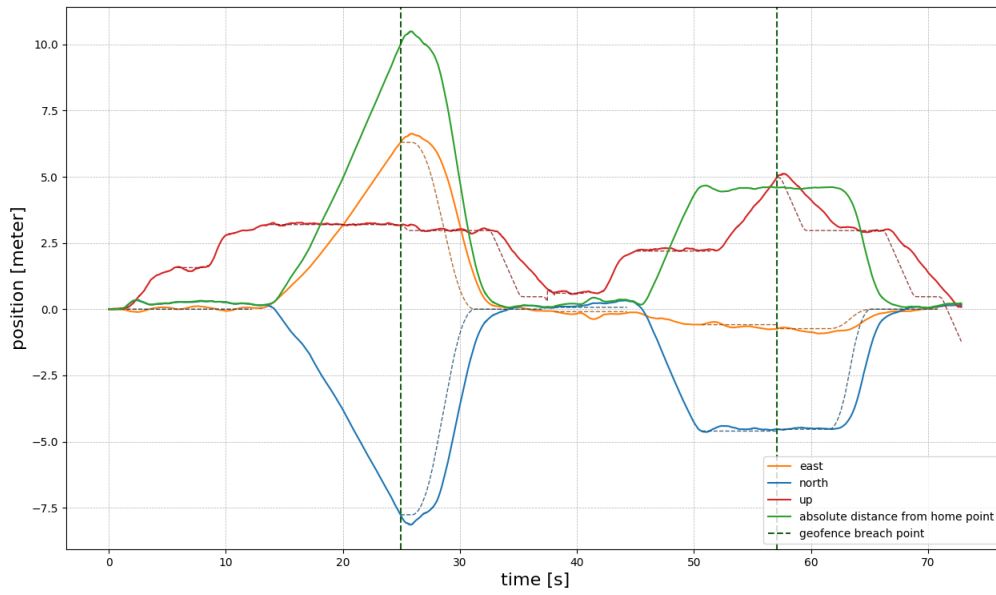
Figure A.11: Geofence breach

8

traj pid
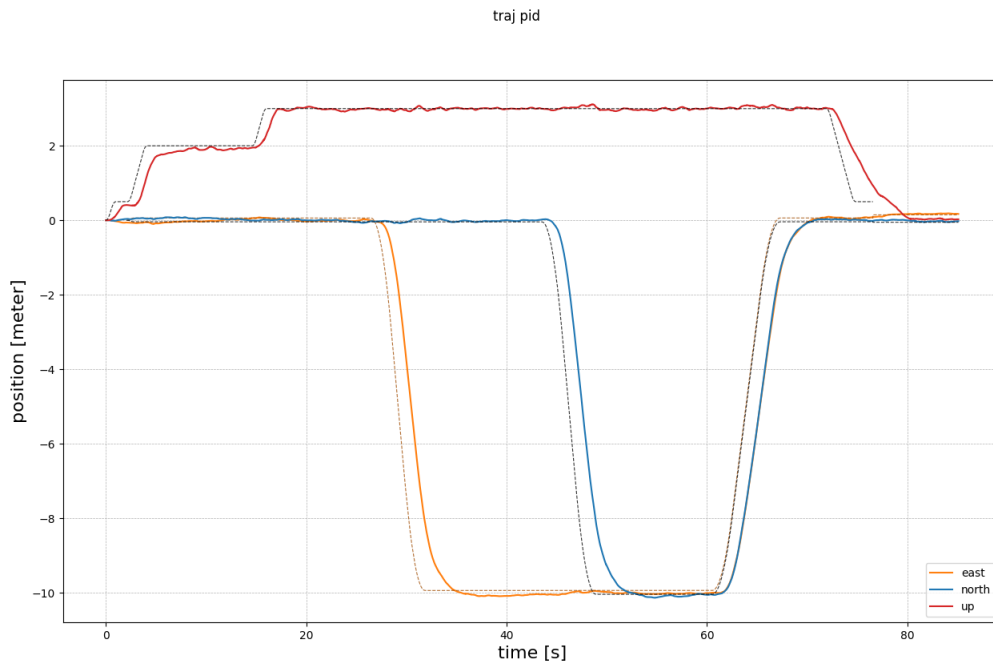
Figure A.12: PID trajectory

traj indi
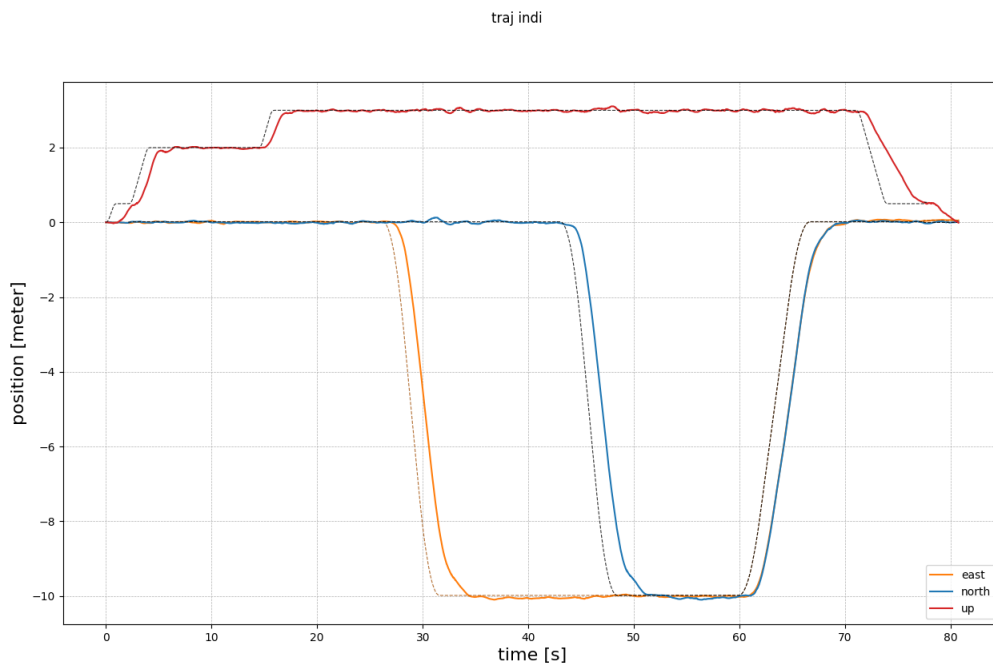
Figure A.13: INDI trajectory

9